



HAL
open science

Rheological and Flow Properties of Gas Hydrate Suspensions

A. Sinquin, T. Palermo, Y. Peysson

► **To cite this version:**

A. Sinquin, T. Palermo, Y. Peysson. Rheological and Flow Properties of Gas Hydrate Suspensions. Oil & Gas Science and Technology - Revue d'IFP Energies nouvelles, 2004, 59 (1), pp.41-57. 10.2516/ogst:2004005 . hal-02017285

HAL Id: hal-02017285

<https://ifp.hal.science/hal-02017285>

Submitted on 13 Feb 2019

HAL is a multi-disciplinary open access archive for the deposit and dissemination of scientific research documents, whether they are published or not. The documents may come from teaching and research institutions in France or abroad, or from public or private research centers.

L'archive ouverte pluridisciplinaire **HAL**, est destinée au dépôt et à la diffusion de documents scientifiques de niveau recherche, publiés ou non, émanant des établissements d'enseignement et de recherche français ou étrangers, des laboratoires publics ou privés.

Rheological and Flow Properties of Gas Hydrate Suspensions

A. Sinquin¹, T. Palermo¹ and Y. Peysson¹

¹ Institut français du pétrole, 1 et 4, avenue de Bois-Préau, 92852 Rueil-Malmaison Cedex - France
e-mail: anne.sinquin@ifp.fr - thierry.palermo@ifp.fr - yannick.peysson@ifp.fr

Résumé — Étude de la rhéologie et des propriétés d'écoulement de suspensions d'hydrate de gaz — La production d'effluents en offshore profond pose un problème important de formation de particules d'hydrate de gaz. En effet, celles-ci peuvent conduire à un bouchage des lignes. Il est primordial de maîtriser cet aspect pour produire ces champs par grande profondeur d'eau. L'article présente différentes actions originales de l'IFP sur le contrôle des écoulements d'hydrate de gaz. Les développements d'additifs « antiagglomérant » ou la présence de tensioactifs naturels permettant de maintenir une dispersion des cristaux d'hydrate sont très prometteurs pour les champs complexes où les techniques classiques de prévention, comme l'isolation ou l'injection de méthanol, deviennent très difficiles.

L'apparition de particules solides dans la phase liquide modifie les conditions d'écoulement. La perte de charge est contrôlée d'une part par le coefficient de friction pour les écoulements turbulents et par la viscosité apparente de la suspension pour le régime laminaire. Dans une première partie, les propriétés rhéologiques des suspensions d'hydrate sont analysées en fonction de la phase huile. Des expériences en boucle d'écoulement permettent, dans une seconde partie, d'examiner l'effet des particules d'hydrate sur le coefficient de frottement turbulent.

L'effet dû à la présence de particules d'hydrate est analysé en termes de comportement rhéologique du système en régime laminaire et en termes de modification du coefficient de frottement en régime turbulent.

Abstract — Rheological and Flow Properties of Gas Hydrate Suspensions — The problem of hydrate blockage of pipelines in offshore production is becoming more and more severe with the increase of the water depth. Conventional prevention techniques like insulation or methanol injection are reaching their limits. Injection of antiagglomerant additives and/or presence of natural surfactants in crude oils give us a new insight into hydrate prevention methods. Hydrate crystals are allowed to form but size of the particles is limited and transportation within the hydrocarbon phase is possible as a suspension.

Solid particles formation in the liquid modifies the flowing properties. The pressure drop is controlled by the friction factor under turbulent flow conditions or by the apparent viscosity in the case of laminar flow regime. In a first part, the rheological properties of hydrate suspension are analysed depending on the oil phase. Results of flow loop experiments are then reported and allow us to determine the modification of the friction factor under turbulent conditions.

Effect of hydrate particles is analysed in terms of rheological properties of the system in the laminar regime and in terms of friction factor modification in the turbulent regime.

INTRODUCTION

Hydrates are clathrate type crystals in which cages of water molecules are stabilized by host molecules. Discovered in 1810, they stayed a laboratory curiosity until Hammerschmit in 1934 highlighted the fact that light hydrocarbon molecules at high pressure can stabilise these crystals as host molecules. He determined that natural gas hydrates might block gas transmission lines at temperature above the ice point. This discovery marked the beginning of a more pragmatic interest in gas hydrates and the beginning of the modern research era. Since 1970, as oil companies have been producing in more and more unusual environments, such as the north slope of Alaska, Siberia, the North Sea and deeper and deeper ocean (Gulf of Mexico, West Africa or Brazil), hydrate problems have become more and more dreaded.

This article presents first some general properties of hydrate and a rapid overview of the industrial context: the methods used today to predict, prevent and eventually remediate pipeline hydrate blockage. In terms of prevention of hydrate blockage, some new options start to be deployed on field. Among these new ways to control hydrates, the possibility to solve the hydrate problem only by avoiding their agglomeration either by adding some dispersant or

antiagglomerant additives or by taking advantage of natural dispersing properties of some crude oils are mentioned.

Influence of hydrate particles in the fluid on rheological properties and on friction factor modifications is then widely developed in the rest of this article. In a first Section, the viscosity modification caused by the hydrate particles is analyzed and comparisons with hard sphere models are presented. The last Section concerns experimental work on the friction factor determination in turbulent flow regime and the modification of the friction factor due to the presence of solid particles.

1 HYDRATE PROPERTIES

For several decades, the problem of hydrates in petroleum production have been studied worldwide in laboratory and loop test facilities. The objectives were and still are to better understand the mechanism of formation, to characterize the physical properties of hydrates but also to try to develop methods to prevent formation of hydrate plugs. This question has become all the more crucial since deepwater fields have been discovered or brought in production. These fields are perfect candidates to encounter hydrate forming conditions.

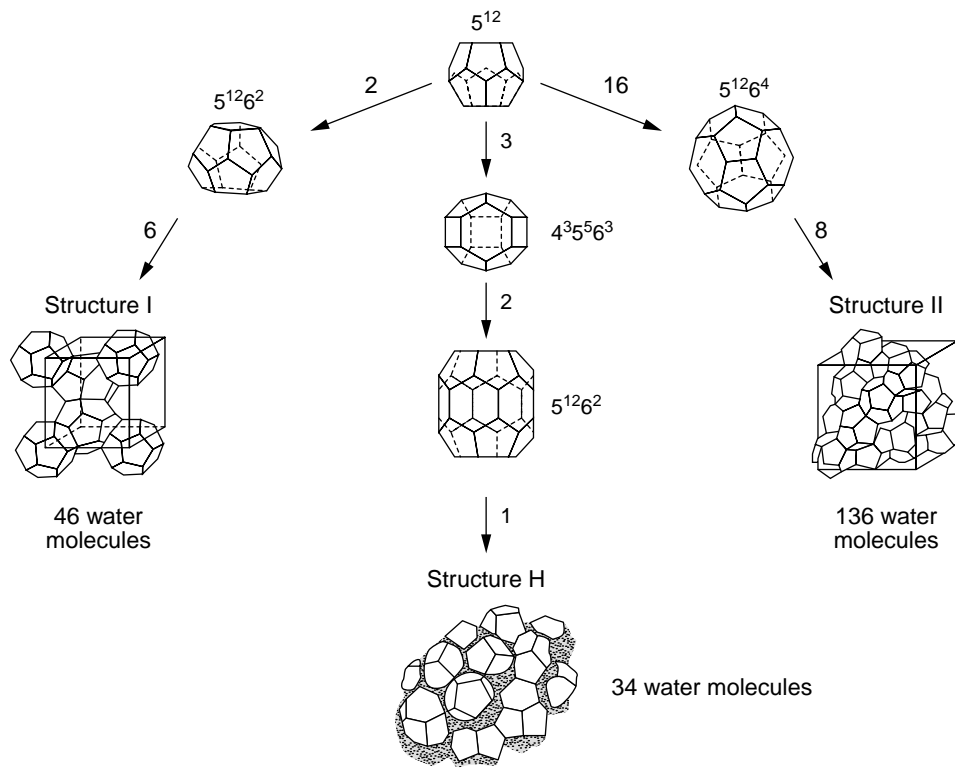


Figure 1

Structure of hydrates (from Sloan [1]).

1.1 Hydrate Structure

Gas hydrates are ice-like crystalline compounds that form whenever water molecules contacts molecules of gas such as low weight molecular hydrocarbon molecules (C_1 , C_2 , etc.) or others: N_2 , CO_2 or H_2S . The hydrate crystals can be thought as a network of hydrogen-bonded water molecules forming cages with gas constituents trapped within. Three different structures have been identified: I, II and H. These structures are illustrated in Figure 1. Structure I and II are constituted by two kinds of cavity: a small one (5^{12}) found in these both structures and a larger one: $5^{12}6^2$ and $5^{12}6^4$ for the structure I and II, respectively. These two structures can be stabilized by molecules of gas having the molecular size in the range 3.5-7.5 Å. For example, the structure I can be stabilized by small gas molecules such as pure methane and pure ethane, but the presence of a small amount of a larger molecule like propane (0.5 mol.%) with methane would result in the formation of structure II. Structure H contains three cavities: the small cage 5^{12} and two large cavities. Molecules as large as cyclopentane can stabilize the larger cavity. However, there is no proof that such structure H hydrates exists in production lines. Consequently, mainly structure II is expected to form with natural gas under production conditions.

1.2 Hydrate Formation

Contrary to ice crystals, gas hydrate crystals are able to form at temperatures higher than $0^\circ C$ as soon as the pressure is higher than a few 10 bar. Conditions promoting hydrate formation are high pressure (typically > 30 bar) and low temperature (typically $< 20^\circ C$). Precise conditions in terms of pressure and temperature depend on composition of the fluids. Hydrate formation can occur for all the produced fluids if required P-T conditions are reached: natural gas, gas condensate and crude with associated gas, with condensed or formation water.

Figure 2 shows curves of dissociation for a natural gas with water and different thermodynamic additives. The dissociation curve delimits, in a P-T diagram, the region where hydrate crystals are thermodynamically stable (stability region on the left side, no hydrate on the right side). The inhibiting effect of salt and methanol at typical concentration used on fields is illustrated. Injection of thermodynamic inhibitor results in a shift of the dissociation curve to the left.

It should be noted that P-T values on the dissociation curve do not necessarily correspond to hydrate formation conditions. At a given pressure, due to "kinetic" effects, the temperature of formation may be shifted down by a few degrees Celsius. This kinetic effect is time dependant, so hydrate will not form at a given pressure and temperature inside the metastable zone during a certain period of time. A more or less wide metastable zone can be drawn (Fig. 2).

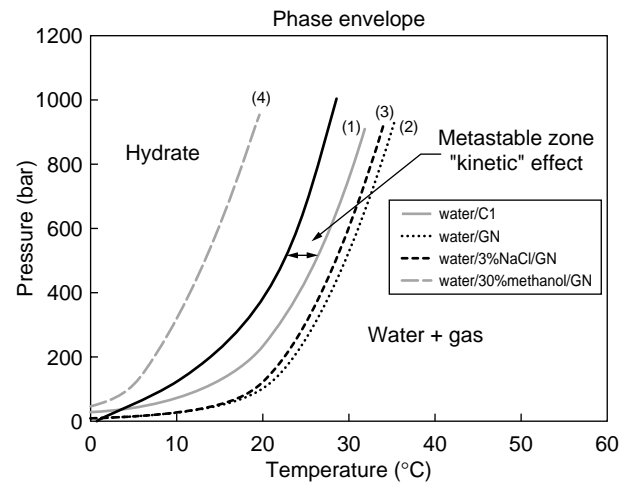


Figure 2

Typical hydrate dissociation curves.

- (1) Methane - structure I;
- (2) Natural gas with 87.5 mol% C_1 , 7.6 mol% C_2 , 3.1 mol% C_3 , 1.2 mol% nC_4 and 0.6 mol% nC_5 - structure II;
- (3) Natural gas and salt water (3 wt% NaCl);
- (4) Natural gas and water + 30 wt% methanol.

This temperature offset normally refers as subcooling. The magnitude of the subcooling depends on the time, the pressure, the flow conditions as well as the composition of the fluids. The higher the subcooling, the shorter the time of hydrate formation and the faster hydrate crystals will grow.

Formation of hydrate particles generally leads, by forming solid plugs, to the blockage of pipelines and thus to the shutdown of production facilities. Hydrate plugs can be the result of growth of deposits on the inner wall and/or agglomeration of hydrate crystals in the bulk. The removal of hydrate plugs is generally difficult to achieve. A shutdown of several days may be necessary prior to the restarting of the production and, indeed, pipeline abandonment may occur. General discussions on hydrate properties can be found in the literature [2-5].

2 INDUSTRIAL CONTEXT

To anticipate and solve potential production problems related to hydrate blockages, operators dispose of tools and means with respect to:

- prediction;
- prevention;
- remediation.

2.1 Prediction Methods

Prediction methods essentially consist in performing thermodynamic calculations that enable dissociation curve of

hydrates to be determined (*Fig. 2*). Even if hydrate formation may actually occur at a lower temperature (or at a higher pressure), from a more practical point of view, the dissociation curve is usually considered as the boundary that must not be passed through. Today, computer models are commercially available on the market and are considered as relatively reliable. However, they necessitate an accurate compositional analysis of the fluids. Risk of hydrate formation can then be definitively evaluated according to pressure and temperature in the lines. It should be noted that accuracy of temperature prediction in pipes is often questionable. This may cause an under or over-estimate of the jeopardy.

2.2 Prevention Methods

2.2.1 To Produce Outside the Hydrate Stability Zone

One way to prevent hydrate blockages is to maintain the pressure and temperature conditions outside the hydrate formation region (delimited by the dissociation curve). This can be accomplished by insulating, burying or heating pipelines to reduce heat losses between the hot produced fluids and the cold environment of the pipeline. This can also be accomplished by shifting the dissociation curve toward the lowest temperatures with the injection of thermodynamic inhibitors such as methanol or glycol (*Fig. 2*).

The most common methods presently used or foreseen by operators are the insulation and the injection of thermodynamic inhibitors. However, both of these solutions have a significant economical impact and a technical limitation.

In addition to its high Capex level and the technical challenge faced by the design and installation of high performance insulation, it will not prevent entering the hydrate formation region during a long-term shutdown. Consequently, additional methods have to be anticipated for shutdown/restart procedures. Nevertheless, it generally prevents hydrate formation during normal operation conditions and simultaneously avoids potential wax deposit formation.

Injection of thermodynamic inhibitors is only effective at high concentration with respect to the water amount (30 to 50 wt%). Methanol injection leads to a high Opex level and also needs large size storage facilities. As for glycol injection, it needs installation of reboilers for glycol regeneration as well as storage requirements accounting for typical loss [6, 7]. Moreover in Gulf of Mexico, the refineries tend now to limit the methanol concentration allowed in the oil and condensate which cause serious problem in desalting operation and water management. Similarly, severe penalties are now applied on the gas containing too much methanol.

2.2.2 New Options: LDHI and/or Natural Surfactants

A new option would be the injection of the so-called “low dosage hydrate inhibitors” (LDHI). Injection of LDHI in place of thermodynamic inhibitors has been considered as the

most interesting option regarding new methods to prevent hydrate blockages and has been subjected to a lot of research works for the last ten years [8-11]. The required concentration for these additives is expected to be less than 1 wt% (with respect to the water amount). Although low concentration can lead to a significant reduction of processing costs, the most interesting issue would probably be the reduction of size storage facilities.

There are two types of LDHI: the “kinetic inhibitors” (KI) and the “dispersant additives” also called “antiagglomerant additives” (AA).

Kinetic inhibitors act by delaying hydrate nucleation and by slowing down crystal growth. Therefore, they do not have any effect on the dissociation curve but avoid, during a finite period, the formation of large hydrate crystals inside the hydrate stability envelope. The applicability of KI is limited by a maximum subcooling at a given residence time in the system. For the last generation of KI, it is commonly admitted that the maximum subcooling temperature is around 10°C for a residence time of 2 days. This limitation appears to be close to the theoretical limit for most KI.

Contrary to thermodynamic inhibitors and kinetic inhibitors, the concept of dispersant additives or AA [12] do not prevent the formation of hydrate crystals but make their transport in suspension feasible by preventing hydrate deposition and formation of large aggregates. Today, AA have mainly limitations in terms of water cut. The maximum water cut is expected to be between 40 and 50%. This limitation is caused by the rheological properties of suspensions with high solid fraction and may depend on flow regime conditions.

Potentiality of LDHI has been highlighted under field conditions [13, 14]. Three fields of the Eastern Trough Area Project (ETAP) in the United Kingdom Central North Sea are currently operating using KI [15]. The Popeye field has used the AA technology [16] and several other projects of AA are studied in Gulf of Mexico and North Sea [17]. For one or two years a growing interest has been noted for the LDHI technologies even if they are not yet extensively used.

In case of black crude oils, instead of injecting additives, it is also expected to have benefits of the presence of “natural surfactants”, such as resins and asphaltenes. Indeed, these compounds are suspected to be able to transport hydrate particles in suspension as dispersant additives or AA do [18, 19]. Consequently, up to moderate water cut, treatment for hydrate control would not be necessary.

2.2.3 Remediation Method

Even if new methods to remove hydrate blockages have been discussed in the literature [20, 21], the method successfully implemented so far by operators is two-sided depressurization [6] (eventually made more effective by injecting methanol or external heating). However, this method may be very time consuming and necessitates reinvestment of

facilities to access plugs from both sides. It may be not practical to depressurize both sides of a hydrate blockage (particularly when several plugs are formed simultaneously in the line). Thus, a one-sided depressurization procedure, resulting in a substantial pressure drop across the plug, has to be deployed [22]. In such a case, two extreme events can occur: firstly, the plug can be extended because of a cooling effect (Joule-Thompson effect) possibly generated by the gas flow through the plug. Secondly, the plug can be suddenly broken off from the pipe wall and flies down the flowline, thus injuring persons or damaging downstream facilities [23].

Since remediation methods are still too much hazardous, efforts are mainly focused on the deployment of prevention methods. From these, the study of the rheological behaviour of real produced fluids in the hydrate stability zone and the influence of hydrate particles on the flow properties become very important.

3 HYDRATE SUSPENSIONS RHEOLOGY

In this Section, we will discuss the rheological behaviour of hydrate suspensions. Such systems are defined, here, as composed of hydrate particles dispersed in a hydrocarbon liquid phase (oil or condensate).

Hydrate formation in a pipeline generally leads to an increase of the pressure drop. In worst situations, it is associated with the growth of plugs and/or deposits, which can lead to a complete blockage of the line. In this case, the system is not homogeneous and an investigation in terms of rheology cannot be achieved. In best situations, in particular thanks to natural surfactants or AA-type LDHI's as previously mentioned, hydrates can be dispersed in the hydrocarbon liquid phase. In this case, the pressure drop may be controlled by the friction factor under turbulent flow conditions (this point will be discussed in the next Section), or by the apparent viscosity of the suspension under laminar flow conditions.

Mainly in collaboration with oil companies as *Petrobras* in Brazil and *Total* in France, *IFP* has been investigating for some years the rheological properties of hydrate suspensions formed in different hydrocarbon liquid phases such as asphaltenic crude oils, acidic crude oils, or condensate + AA's. These investigations have been performed in two homemade devices: a laboratory rheological P-T cell [19] and a multiphase pilot loop [24]. The pilot loop will be briefly described later. Depending on the oil phase system, different results have been obtained. Systems exhibit shear-thinning properties whereas others can be well described as Newtonian suspensions. The relative viscosity, defined as the apparent viscosity divided by the viscosity of the oil phase, can also vary by one or two orders of magnitude from a system to another one.

In the following, we will remind results obtained for hydrate suspensions in an asphaltenic crude oil as well as a

phenomenological model developed in order to describe rheological properties of such suspensions. These results have been presented in several former papers [19, 24-26] that the reader is invited to refer for more details. Based on an analysis of forces of interaction between hydrate particles as well as results obtained with other systems, a general discussion on expected rheological properties of hydrate suspensions is then presented.

3.1 Hydrate Suspensions in an Asphaltenic Crude Oil

3.1.1 General Properties

This crude oil is a rich asphaltenes-containing crude (around 5 wt%). It allowed us to form very stable water in oil emulsions. Under typical shear stress conditions encountered in real transportation conditions, water droplet diameters have been measured in the range of 0.5 to 3 μm . Moreover, no significant change in size has been noticed before hydrate formation and after hydrate dissociation. The crude oil also showed a very good capability in transporting hydrate particles as a suspension and made rheological investigations feasible. As showed by Camargo *et al.* [19, 24], shear-thinning and time-dependant (thixotropy) properties were observed for hydrate suspensions for a volume fraction of 0.27 and above. On the other hand, suspensions formed at a volume fraction of 0.134 behaved roughly like Newtonian fluids.

For this system, it was expected, in first approximation, that a hydrate particle was formed from an individual water droplet without any significant change neither in size (the volume expansion due to hydrate formation is neglected) nor in form (roughly spherical). Thus, based on general theories related to rheology of hard-sphere dispersions, a phenomenological model has been developed by Camargo and Palermo [26] as an attempt for understanding and predicting rheological properties of hydrate suspensions.

3.1.2 Phenomenological Model

Up to a particle volume fraction Φ around 0.5, a monodisperse hard-sphere suspension is a fluid for which the viscosity is a function of Φ as well as the dimensionless shear stress:

$$Pe = \frac{\tau \left(\frac{d_p}{2} \right)^3}{k_B T}$$

where τ is the actual shear stress, $d_p/2$ the particle radius and $k_B T$ the thermal energy. In the limits of both low stresses and high stresses, the viscosity depends only on the volume fraction. For stresses conditions around $Pe = 1$, shear thinning occurs and the viscosity depends also on the size of the particles. By considering radius of hydrate particles larger than 1 μm and typical shear stresses in realistic flow conditions

much larger than 1 Pa for the hydrate/crude oil system (suspension viscosity $\mu \gg 0.01$ Pa·s; shear rate $\dot{\gamma} > 100$ s⁻¹), we have $Pe \approx 10^2 \gg 1$. We can then consider that, in our case, the contribution of hydrodynamic interactions dominates with respect to the contribution of the Brownian motion and should confer to the hydrate suspension a Newtonian behaviour (high stresses limit).

However, shear thinning is frequently observed for concentrated suspensions. This phenomenon, particularly when it is associated with a thixotropic behaviour, is generally attributed to a reversible aggregation process that takes place between particles under shear flow.

Let us first consider viscosity laws of concentrated suspensions. Generally, equations are expressed as relationships between the relative viscosity μ_r and the couple (Φ, Φ_{\max}) . The relative viscosity is the ratio between the apparent viscosity μ of the suspension and the viscosity of the dispersing liquid μ_0 . Φ is the particle volume fraction and Φ_{\max} is physically interpreted as the maximum volume fraction to which particles can pack. We will use the equation proposed by Mills [27], well adapted to hard spheres of equal size and accounted only for hydrodynamic interactions:

$$\mu_r = \frac{1 - \Phi}{\left(1 - \frac{\Phi}{\Phi_{\max}}\right)^2}; \Phi_{\max} = \frac{4}{7} \quad (1)$$

Φ_{\max} is taken as the packing concentration of randomly packed spheres of same diameter.

Let us now consider aggregated suspensions. Several theoretical models have been proposed in the literature [28, 29] to describe the growth of particle clusters either by perikinetic aggregation (caused by Brownian motion) or by orthokinetic aggregation (caused by medium flow). The porosity of the resulting aggregates is taken into account by introducing a fractal dimension fr , relating the number of particles N per fractal aggregate to characteristic lengths of the system (d_A : aggregate diameter; d_p : particle diameter):

$$N = \left(\frac{d_A}{d_p}\right)^{fr} \quad (2)$$

Depending on the type of the characteristic length d_A , a prefactor can be introduced in the former relationship. As demonstrated by Gmachowski [30], this prefactor is equal to unity if d_A corresponds to the “dynamic” diameter, the one that should be taken into account with respect to hydrodynamic phenomena. Due to the fractal structure of aggregates, it has been proposed that an effective particle volume fraction Φ_{eff} should be considered instead of the real volume fraction in the expression for the viscosity [27]:

$$\mu_r = \frac{1 - \Phi_{\text{eff}}}{\left(1 - \frac{\Phi_{\text{eff}}}{\Phi_{\max}}\right)^2}; \Phi_{\max} = \frac{4}{7} \quad (3)$$

with:

$$\Phi_{\text{eff}} = \Phi \left(\frac{d_A}{d_p}\right)^{(3-fr)} \quad (4)$$

It is well accepted that the fractal dimension, for perikinetic aggregation, ranges from about 1.7 to 2.1. Under shear conditions, it is generally reported that aggregates are more compact with fractal dimension larger than 2 and up to 2.7 [31].

Because of viscous forces applied on aggregates in the flow, they cannot grow indefinitely. A maximum size is reached depending on the balance between the shear stress and the force of adhesion F_a between particles. By considering a mechanism of destruction based on the erosion of microflocs [32], the maximum size of aggregates for laminar flow is given by:

$$d_{A,\max} = \left[\frac{F_a (d_p)^{2-fr}}{\mu_0 \dot{\gamma}} \right]^{\frac{1}{4-fr}} \quad (5)$$

where $\dot{\gamma}$ is the shear rate.

In Equation (5), the shear stress exerted to aggregates is related to the viscosity μ_0 of the dispersing liquid. It is only correct when aggregates do not interact, *i.e.*, $\Phi \rightarrow 0$. However, for finite Φ , hydrodynamic interaction of aggregates can be taken into account, as proposed by Potanin [29], by substituting in Equation (5) the viscosity μ_0 by the apparent viscosity of the suspension μ . Finally, we have:

$$d_{A,\max} = \left[\frac{F_a (d_p)^{2-fr}}{\mu \dot{\gamma}} \right]^{\frac{1}{4-fr}} \quad (6)$$

At the equilibrium, we consider that $d_A \sim d_{A,\max}$. Combining Equations (3, 4 and 6) d_A/d_p can be determined by solving the following equation:

$$\frac{d_A^{(4-fr)}}{d_p} - \frac{F_a \left[1 - \frac{\Phi}{\Phi_{\max}} \left(\frac{d_A}{d_p}\right)^{(3-fr)} \right]^2}{d_p^2 \mu_0 \dot{\gamma} \left[1 - \Phi \left(\frac{d_A}{d_p}\right)^{(3-fr)} \right]} = 0 \quad (7)$$

If the solution of Equation (7) is $d_A/d_p < 1$, d_A is fixed equal to d_p . The relative viscosity is then determined by using Equation (3).

3.1.3 Comparison between Model and Experiment

Results obtained from the phenomenological model are compared in Figure 3 with some experimental results obtained for hydrate suspensions formed with the asphaltenic crude oil.

Except for the force of attraction F_a , all the parameters have been set to their assumed or measured value.

According to the discussions above, the fractal dimension has been set to $fr = 2.5$, the maximum packing concentration to $\Phi_{\max} = 4/7$, and the particle diameter to $d_p = 1.5 \mu\text{m}$. The viscosity of the continuous oil phase corresponding to the experimental conditions (pressure: 7.5 MPa; temperature: 7.5 °C) is $\mu_0 \approx 60 \text{ cP}$.

Experimental results are presented for two particle volume fractions: $\Phi = 0.134$ and $\Phi = 0.274$. Due to time-dependant properties of suspensions, only results obtained during the increase of the shear rate are shown. Indeed, it is expected that the destruction of aggregates is a more rapid process than formation. Consequently, the relative viscosity measured under such conditions is probably closer to the equilibrium state than the one measured during a decrease of the shear rate.

Results of calculation correspond to a force of attraction: $F_a = 1.2 \cdot 10^{-9} \text{ N}$. Expressed with respect to the radius of curvature of the surface $d_p/2$, we have $2F_a/d_p = 1.6 \text{ mN/m}$.

Globally, the evolution of the relative viscosity with the shear rate, depending on the particle volume fraction, is well described by the aggregation model. At low volume fraction ($\Phi = 0.134$), calculation indicates that the increase of the relative viscosity should be only significant at low shear rates (below 50 s^{-1}). Experimentally, in the range of shear rates investigated (50 to 600 s^{-1}) neither shear thinning nor thixotropic behaviour have been observed. At $\Phi = 0.274$, we have a good agreement between calculation and experimental data with a shear-thinning behaviour well described.

For such aggregated suspensions, it has been showed that the rheological behaviour can be well described by a Casson's like equation of the form: $\tau^{1/2} = \tau_0^{1/2} + (\alpha\dot{\gamma})^{1/2}$ where τ is the shear stress, τ_0 the yield stress, and α a constant, which slightly depends on Φ .

3.2 Forces of Interaction between Hydrate Particles

Camargo and Palermo [26] also discussed the origin of forces involved in hydrate particle interactions. The authors argued that van der Waals forces were too weak to explain aggregation in the asphaltenic crude oil. On the other hand, they suggested that, due to adsorption of asphaltenes, interactions between hydrate particles in the asphaltenic crude oil might be similar in nature to the ones encountered between polymer-covered surfaces.

3.2.1 Effect of van der Waals Forces on Rheological Behaviour of Hydrate Suspensions

As van der Waals forces always exist in disperse systems, it is of interest to analyse how they are able, in the absence of other forces, to promote aggregation, and consequently promote a shear thinning behaviour, depending on the characteristics of the system.

The van der Waals forces between two spheres of same radius $d_p/2$ is given by the relation [33].

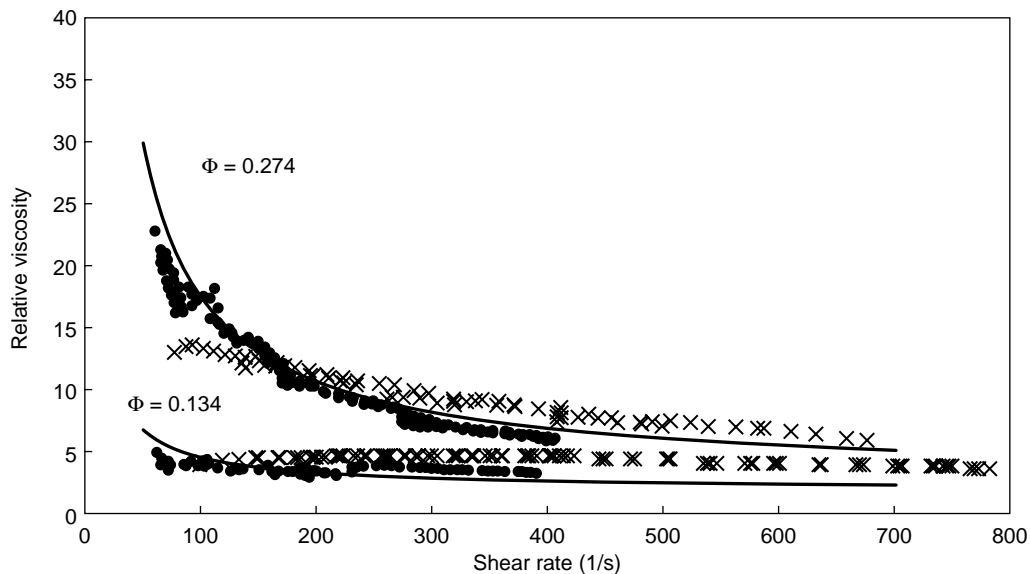


Figure 3

Comparison between calculation and experimental data obtained for hydrate suspensions in the asphaltenic crude oil. Lines: calculated from the model; marks: experimental data obtained in the loop (\bullet) and in the cell (\times) - (from Camargo and Palermo [26]).

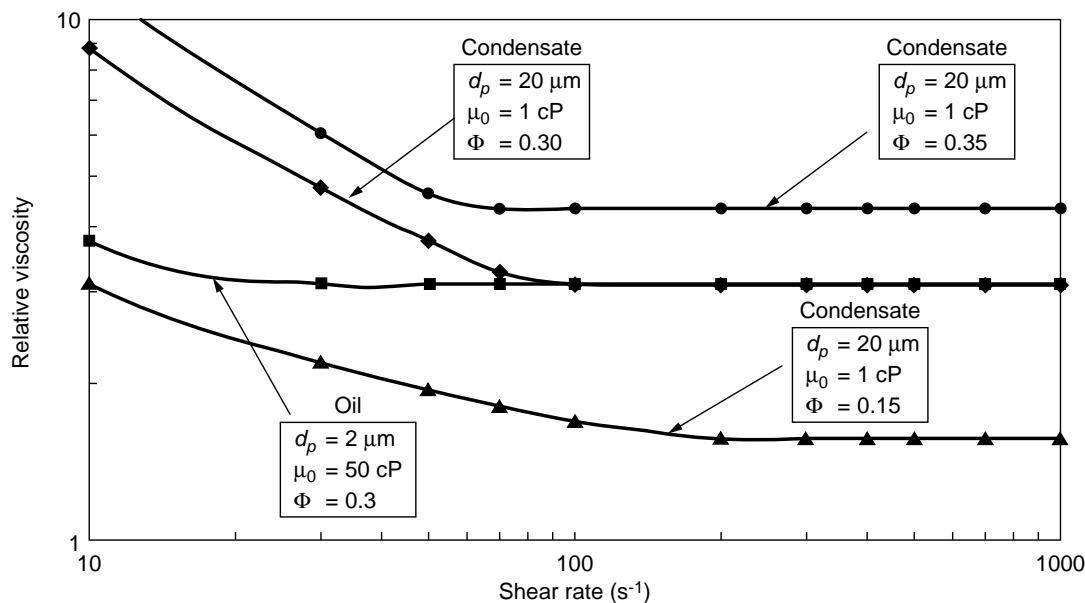


Figure 4

Calculation of the relative viscosity as a function of the shear rate for two expected limit cases corresponding to condensate and oil phase systems.

$$F_a = \frac{A(d_p/2)}{12d_s^2} \quad (8)$$

where A is the Hamaker constant and d_s the distance which separates the two spheres. For hydrate particles dispersed in an oil phase, A has been estimated around $5.2 \cdot 10^{-21} \text{ J}$ [26]. Accounting for a surface roughness of particles larger than 50 \AA which maintain particles at a distance $d_s > 50 \text{ \AA}$, $2F_d/d_p$ falls down rapidly below 0.01 mN/m .

Calculation of the relative viscosity as a function of the shear rate is illustrated in Figure 4 depending on the volume fraction Φ , the viscosity of the oil phase μ_0 and the diameter of hydrate particles d_p . The term related to van der Waals forces has been set to $2F_d/d_p = 0.01 \text{ mN/m}$, that is expected to correspond to the upper limit. The more uncertainties are about the size of hydrate particles. Few data have been reported in the literature. Measurement of size of hydrate crystals formed in a water continuous phase indicates that crystals rapidly growth above 10 \mu m [34]. In case size of hydrate particles are limited to the size of water droplets dispersed in the oil phase, it is expected to have a radius in the range of some \mu m (viscous or rich surfactant-containing crude oil) to tens of \mu m (light crude oil, condensate).

Two expected limit cases are illustrated: $d_p = 2 \text{ \mu m}$, $\mu_0 = 50 \text{ cP}$ at $\Phi = 0.3$, and $d_p = 20 \text{ \mu m}$, $\mu_0 = 1 \text{ cP}$ at $\Phi = 0.15$, 0.3 and 0.35 , corresponding to a crude oil system and a

condensate system, respectively. For the condensate system, we can see that a shear-thinning behaviour, associated with an aggregation process of hydrate particles, might be only visible at low shear rate ($< 100 \text{ s}^{-1}$). As the volume fraction increases, deviation from the Newtonian regime occurs at lower shear rates and shear thinning increases in magnitude. For the crude system, even for smaller particles, the increase in viscosity of the oil phase keep the suspension as Newtonian down to a shear rate of 10 s^{-1} .

The actual wall shear rate in real conditions can be estimated from the Hagen-Poiseuille law (Newtonian approximation): $\dot{\gamma}_w = 8U/D$ where U is the real mean liquid velocity and D is the pipe diameter. U is usually in the range of 2 to 5 m/s for oil production and even larger for condensate. By taking D of the order of 0.1 m , we have $\dot{\gamma}_w \geq 100 \text{ s}^{-1}$. Let us remind that numerical values chosen above correspond to limit cases. It is consequently expected that hydrate suspensions behave as Newtonian fluids under normal conditions of production if only van der Waals forces are involved in the interaction between hydrate particles. Only for extreme limit cases gathering small particle radius, low oil viscosity, high particle volume fraction, large pipe radius and low velocity, shear-thinning behaviour should be expected. Note that in this case, particularly for low viscosity and low velocity, other phenomena as particle sedimentation might occur which make rheology a nonpertinent approach to predict flow properties.

3.3 Hydrate Suspensions in Other Systems

3.3.1 Rheological Behaviour

We present below results obtained for two other systems. The first one (Fig. 5) concerns a hydrate suspension formed in an acidic crude oil (Dalia 3) at a water cut of 27 vol%. It should be noticed that, in contrast to the previous crude oil, Dalia 3 crude oil contains less than 1 wt% of asphaltenes. The second one (Fig. 6) corresponds to a hydrate suspension formed with a condensate + AA-type LDHI at a water cut of 40 vol%. Results are presented in terms of nondimensional friction factor $f = (\Delta P/L)/2\rho U^2$ and Reynolds number $Re = \rho U D/\mu_0$ where ρ , U et μ_0 are respectively the density, the velocity and the dynamic viscosity of the crude, $\Delta P/L$ the pressure gradient, and D the pipe diameter.

In the laminar regime, it can be seen that the two systems exhibit a Newtonian behaviour. This confirms that a Newtonian behaviour should be expected for hydrate suspensions as far as other forces than van der Waals forces are not involved in the interaction between hydrate particles.

3.3.2 Relative Viscosity

In Table 1, relative viscosities of hydrate suspensions are reported for the different oil systems mentioned above and at different volume fractions. Results for the asphaltenic crude oil are also indicated. In this last case, the relative viscosity corresponds to the one measured at high shear rate (700 s^{-1}) for which it is predicted that aggregates consist of a few hydrate particles. Moreover, experimental values are compared with calculated values according to Equation (1)

for the Newtonian suspensions and Equation (3) for the aggregated suspension.

For hydrate suspensions formed in the asphaltenic crude oil, the relative viscosity remains at the same order of magnitude as the calculated one. This confirms that hydrate suspensions can be considered, in first approximation, as hard-sphere dispersions. Discrepancies between experimental and calculated values are in the range of experimental error but may also be the result of the volume expansion of particles associated with hydrate formation and a slight deviation from the ideal spherical shape.

On the other hand, for the other systems, discrepancies of one or two orders of magnitude between experimental and theoretical values indicate that the former assumption is no longer valid. Note that the higher the initial water cut, the larger the discrepancy. It is suspected, for such systems, that hydrate particles are strongly different in shape and size from initial water droplets. Particles probably stem from the agglomeration of primary particles, such a process occurring during hydrate formation. It has been suggested by some authors [26, 36] that capillary forces, associated with the presence of free water during this stage, are responsible for this agglomeration process. Resulting hydrate particles are therefore large and porous particles, contributing to an increase of the effective volume fraction. Contrary to the reversible aggregation mechanism observed with the asphaltenic crude oil, such an agglomeration process is not reversible. The effective volume fraction does not depend on the shear rate and the relative viscosity remains at a high level whatever the flow rate.

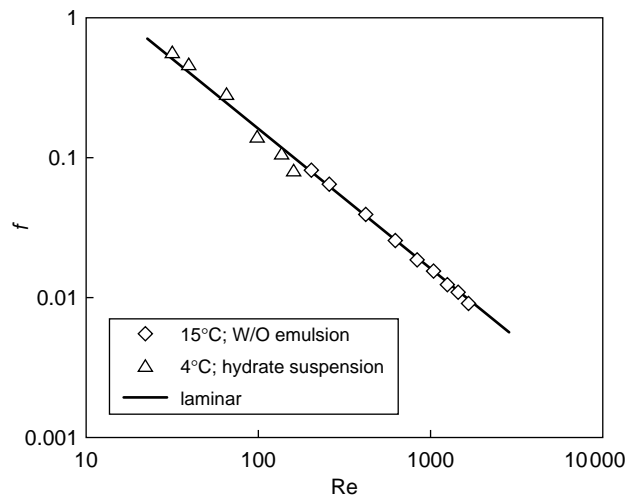


Figure 5

Characterization of emulsion and hydrate suspension at 30 wt% of water cut for Dalia 3 crude oil (from Maurel *et al.* [35]).

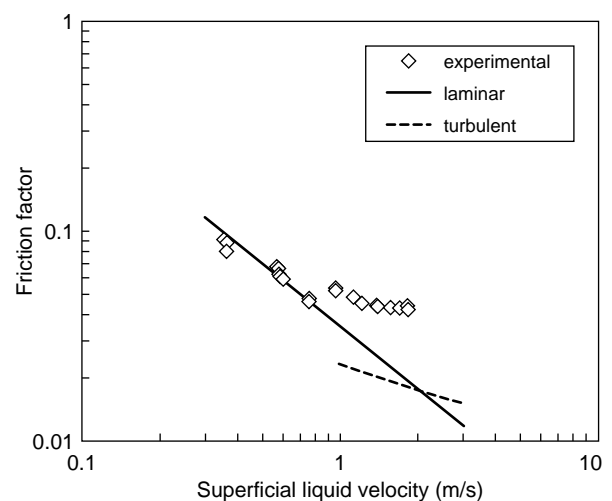


Figure 6

Characterization of hydrate suspension at 40 wt% of water cut for condensate + AA additive (from Camargo [25]).

TABLE 1
Relative viscosity of hydrate suspensions for different oil systems

Oil phase	Initial water cut	Relative viscosity exp. / (calculated)	References
Condensate + AA	0.2	4.2 / (1.9) - Eq. (1)	Camargo [25]
	0.3	38.5 / (3.1) - Eq. (1)	Camargo [25]
	0.4	69.2 / (6.7) - Eq. (1)	Camargo [25]
Dalia 3	0.27	10 / (2.6) - Eq. (1)	Maurel <i>et al.</i> [35]
Asphaltenic crude oil (at high shear rate)	0.134	3.8 / (2.24) - Eq. (7)	Camargo and Palermo [26]
	0.274	5.9 / (5.11) - Eq. (7)	

Because of the large size of hydrate particles (larger than $1\ \mu\text{m}$) and the weakness of van der Waals forces, hydrate suspensions are non-Brownian dispersions for which a Newtonian behaviour is expected. In some particular cases, for which heavy compounds as asphaltenes are able to adsorb on hydrate surface and generate polymer-like interactions, a reversible aggregation process can take place and a shear-thinning behaviour can be observed.

Prediction of viscosity of hydrate suspensions could be achieved with the help of hard-sphere dispersion models. However, difficulty in quantitatively predicting the viscosity arises from the fact that hydrate particles may form from the agglomeration of primary particles during the hydrate formation stage. This agglomeration process promotes the formation of large and porous particles and results in a strong increase of the effective particle volume fraction.

4 TRANSPORT OF HYDRATE DISPERSED IN PIPE

In field conditions, the single phase or multiphase flow in pipelines leads to pressure drops controlled by the friction factor of the fluids. In the laminar case, the friction factor is related to the viscosity and determination of the rheology allows the pressure drop estimation. The previous Section discussed in details this issue. In this Section, we will focus on turbulent friction factor and the effect of hydrate particle on their determination. This determination is only possible through flow loop experiments.

The experimental procedure consists of the study of different oils flowing in a large flow loop and aims at analysing the modification of the pressure drop when water is added and turned into hydrates in presence of AA-type LDHI's. The modification of the pressure drop for different mean flow rates can be related to the presence of particles.

4.1 Experiments

Experiments were conducted in a multiphase flow loop specially built by the *Institute* to study at a large scale oil and gas flow. A picture of this loop is presented in Figure 7.



Figure 7

Picture of the IFP "lyre" flow loop built to study issues related to multiphase flow of oil and gas.

4.1.1 Flow Loop Characteristics

This flow loop is a horizontal, 2" internal diameter, carbon steel flow line of 140 m long. It has been designed to work in controlled thermodynamics conditions. The temperature can vary from 0 to 50°C and pressure from 1 to 100 bar. A positive displacement pump (flow rate up to 20 m³/h) allows fluid circulation for the liquid phase. A membrane compressor (flow rates up to 2000 Nm³/h) is provided for circulation of the gas phase. In order to keep the pressure constant in the loop, gas is added to it from a gas tank.

Flow rates of each phase, pressures and temperatures at different locations in the flow loop are controlled. More details of the system can be found in Camargo [25] or in Peysson *et al.* [37].

4.2 Flow Characterization

4.2.1 Flow Regime

Flow conditions in pipelines for oil production are dependent on the rheological characteristic of the hydrocarbon phase.

Laminar or turbulent flow regime can be found depending on the apparent shear viscosity.

Typically, pipe diameters are around ~0.1 m and liquid velocity are between 1 and 5 m/s. At 1m/s, a viscosity of 100 cP (0.1 Pa·s) leads to a Reynolds number of the order of magnitude 1000 and flow can be considered laminar. But when viscosity is around 10 cP (0.01 Pa·s), Reynolds number is up to 10 000. So for light oil and condensate, flow regime will be mainly turbulent.

4.2.2 Pressure Drop Calculation

Force balance in steady state for pipe flow (Fig. 8) give the following relation between stress at the wall and imposed pressure drop in the system:

$$\tau_w = \frac{\partial p}{\partial z} \frac{R}{2} \tag{9}$$

Note that this relation is not dependent on the rheology of the system.

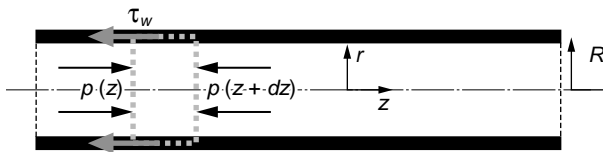


Figure 8
Force balance on a portion of fluid.

In the laminar regime, pressure drop calculation is related to the determination of the apparent shear viscosity of the oil. When viscosity is known (or complete rheology if the fluid is non-Newtonian), pressure drop calculation can be made using the equation of motion (Eq. 9). The problem is to have the rheological knowledge of the system as discussed in the previous Section.

The stress at the wall have a different form when flow regime is laminar or turbulent. But a common expression can be written when introducing the friction factor *f*.

The pressure drop ($\Delta P/L$) in a pipe is then:

$$\frac{\Delta p}{L} = f \cdot \frac{\rho U^2}{R} \tag{10}$$

U is the average velocity of the flow. *R* is the pipe radius, ρ the flowing phase volume mass. *f* is only dependent upon the Reynolds number of the flow define as:

$$Re = \frac{\rho U D}{\mu} \tag{11}$$

μ is the dynamic viscosity of the liquid phase. For Reynolds number less than 2000-3000 the flow is laminar and friction factor can be easily calculated from the Poiseuille velocity profile. We get for Newtonian fluids:

$$f = \frac{16}{Re} \tag{12}$$

f is difficult to estimate in turbulent flow, but different correlations have been proposed with a very good agreement with

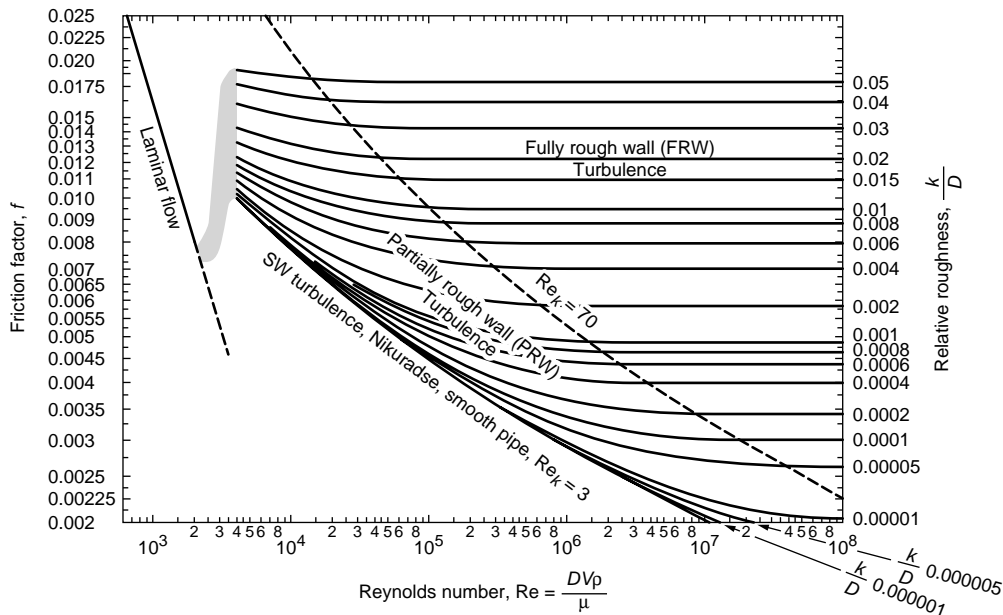


Figure 9
The Moody chart: *f* versus *Re* (from Govier and Aziz [38], p. 167).

the data. The Moody chart of f versus Re is represented in Figure 9. This is the most accepted correlation for f .

As it can be seen in the Moody chart, f is quasi constant for highly turbulent flow. Its value depends essentially from the pipe roughness ε (the mean size of the surface texture). For high Re , f is given by the Nikuradse correlation (see for example Govier and Aziz [38]):

$$\frac{1}{\sqrt{f}} = 4 \log\left(\frac{D}{2\varepsilon}\right) + 3.48 \quad (13)$$

Between Reynolds number $Re = 3000$ and $10\,000$, f exhibits a small dependence with velocity. This dependence of f can be estimated from the Wood-Colebrook law for pipe with intermediate roughness:

$$\frac{1}{\sqrt{f}} = 4 \log\left(\frac{D}{2\varepsilon}\right) + 3.48 - 4 \log\left(1 + 9.35 \left(\frac{D}{2\varepsilon} \cdot \frac{1}{Re \sqrt{f}}\right)\right) \quad (14)$$

In the following, we will focus on flow at large Reynolds number, which is the most encounter flow regime for light oil or condensate.

Different types of fluid have been tested in the “lyre” flow loop. We will focus now on experiments on light oils. Two sets of data will be used. The first one was recorded with a naphtha oil in a large study in collaboration with IFP, IFE, BP, Total, NorskHydro, Shell and Conoco. More details on these experiments can be found in References [37 and 39]. The second was conducted with condensate oil during the PhD, work conducted by Camargo [25].

4.3 Hydrate in Naphtha Oil

4.3.1 Fluids

The first set of experiments was done with light naphtha oil with low viscosity and density. The density of the Naphtha oil saturated with gas (which is the case in the loop) is about 733 kg/m^3 at 25°C and 737 kg/m^3 at 4°C . Naphtha oil viscosity has been measured with a low shear rheometer at atmospheric pressure. The naphtha had a dynamic viscosity of $0.6 \text{ mPa}\cdot\text{s}$ at 25°C and $0.8 \text{ mPa}\cdot\text{s}$ at 4°C . Under pressure conditions (4 MPa), viscosity is expected to be two or three times lower.

Natural gas delivered by the domestic gas network is used in the loop. This gas allows formation of hydrates of structure II.

4.3.2 Hydrate Formation

Naphtha oil and water are mixed together in the test flow loop at 25°C and the AA additive is added. Circulation is done at constant flow rate. Emulsion is quickly formed and

flow conditions become stable in time. After formation of the emulsion in the loop, the loop is cooled down to form hydrates while temperature and gas consumption are monitored. Hydrate formation is detected by the temperature increase as expected from hydrate formation exothermic reaction. Water droplets in the oil phase are turned into hydrate particles. The reaction continues until all accessible water is converted into hydrates.

The flow regime during the hydrate formation period is slug flow. The flow conditions are maintained until the parameters like pressure, temperature are stable with time.

In the loop, the pressure is maintained by addition of gas in the separator. During the hydrate formation stage, gas is used to form hydrate, so gas is injected in the loop to adjust pressure. The monitoring of this consumption can give an indication on the water conversion in the system. This calculation was done, and we get a conversion of roughly 50% of the amount of water in the system. This can be explained by the fact that water droplet are turned into solid particles starting from the outside of the droplet. So a crust is formed, but we can imagine that the core of the solid particles is filled with free water.

4.3.3 Flow

At this stage, after a period of mixing, the pressure drop versus velocity is measured at 4°C for the naphtha oil with hydrate particles. No gas is injected in the loop. The results are shown in Figure 10.

We add on the measurement represented in Figure 10, the calculation of the pressure drop:

$$\frac{\Delta p}{L} = f \cdot \frac{\rho U^2}{R}$$

with a fixed value of f determined experimentally.

4.4 Hydrate in Condensate

4.4.1 Fluids

The hydrocarbon liquid phase chosen is a condensate. Its density is $\rho = 800 \text{ kg/m}^3$. The viscosity is Newtonian and was determined at ambient conditions at $2.8 \text{ mPa}\cdot\text{s}$. But pressurised with gas in the loop, the viscosity of the condensate with saturated gas is around $1 \text{ mPa}\cdot\text{s}$ (this determination is done by considering the pressure drop at low velocities and comparison with Poiseuille law). The same gas as for the naphtha measurements was used.

4.4.2 Flow

The pressure drop versus velocity is also measured at 4°C when hydrate particles are formed. The results are shown in Figure 11.

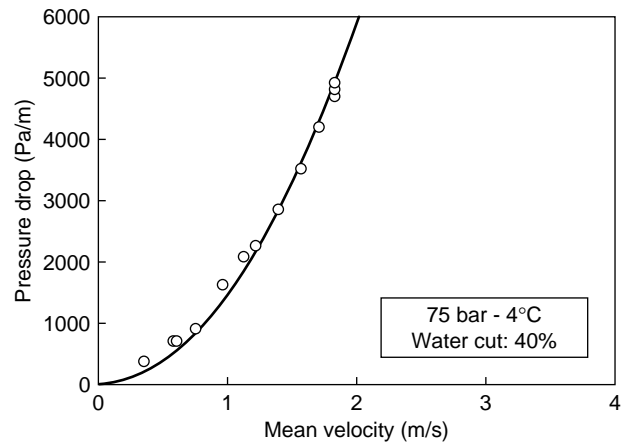
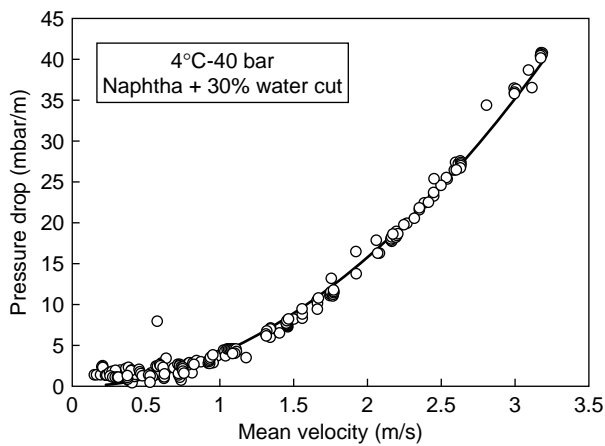
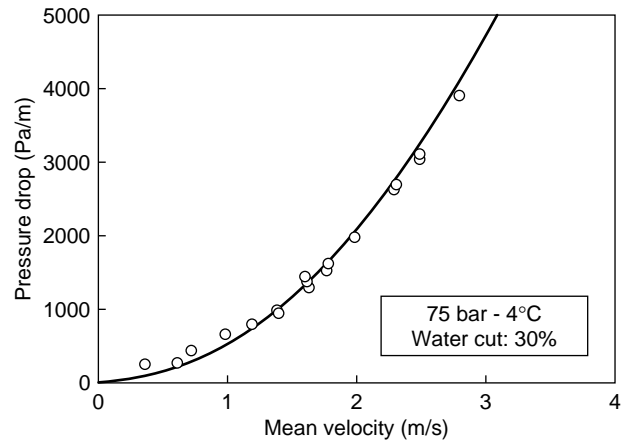
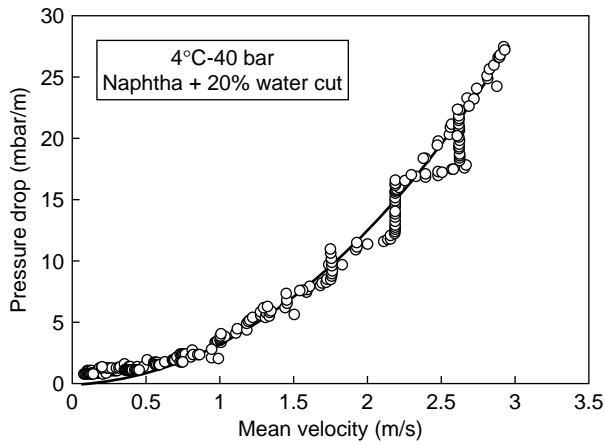
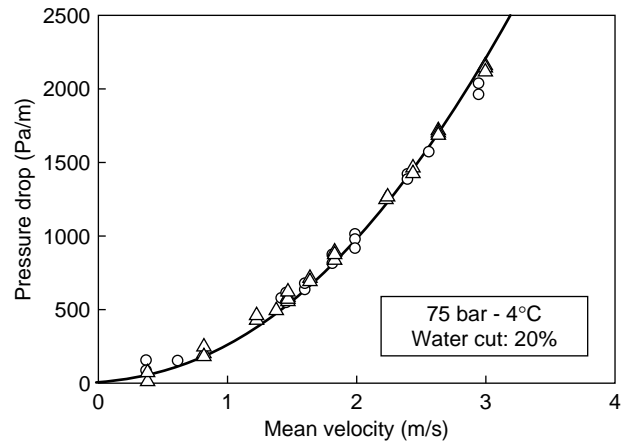
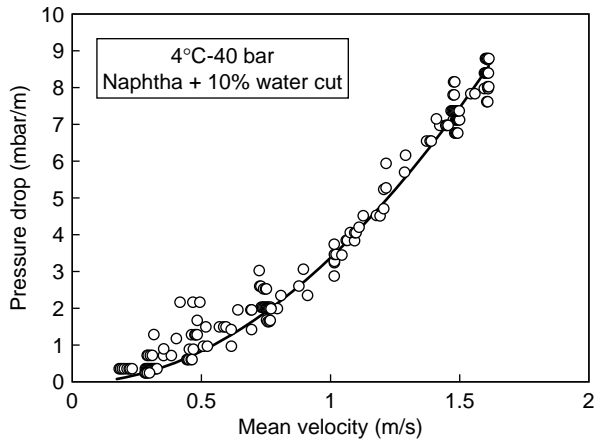


Figure 10

Pressure drop (mbar/m) versus mean velocity (m/s) for naphtha and hydrate particles at different water cut. Line: calculation of the pressure drop in the system with friction factor adjusted.

Figure 11

Pressure drop (Pa/m) versus mean velocity (m/s) for condensate and hydrate particles at different water cut. Line: calculation of the pressure drop in the system with friction factor adjusted.

The black line in Figure 11 is:

$$\frac{\Delta p}{L} = f \cdot \frac{\rho U^2}{R}$$

with a fixed value of f adjusted by best fit on the experimental data.

4.5 Discussions

4.5.1 Friction Factor and Flow Regime

For both systems, naphtha and condensate, we observe a good agreement between the data and the calculation especially for velocities more than 1 m/s confirming that the flow regime is turbulent and f is constant. This is confirmed in Reynolds number calculation. Indeed, in the two system, the viscosity of the fluid is very low (0.5 mPa·s for naphtha oil

and 2.8 mPa·s for condensate or more close to 0.2 and 1 mPa·s, respectively, in the pressured case). The difficulty in Reynolds number calculation with hydrates in the fluid is that the viscosity of the effective media (hydrate suspension) is not so well defined.

In order to get rid of this difficulty, we can plot the pressure drop *versus* velocity in a log-log plot. Indeed, linear increase with velocity is characteristic of laminar flow and square like dependency is the one of turbulent flow. Equation (10) shows that for turbulent flow, $\Delta P/L$ scales as U^2 (f does not depend on velocity). In laminar flow, $\Delta P/L$ scale as U (Poiseuille flow $\Delta P/L = \mu \cdot (8/\pi) \cdot U/R^2$).

4.5.2 Variation of f with Water Cut

As discussed in the former section, particularly for the condensate + AA system, hydrate particles may form from

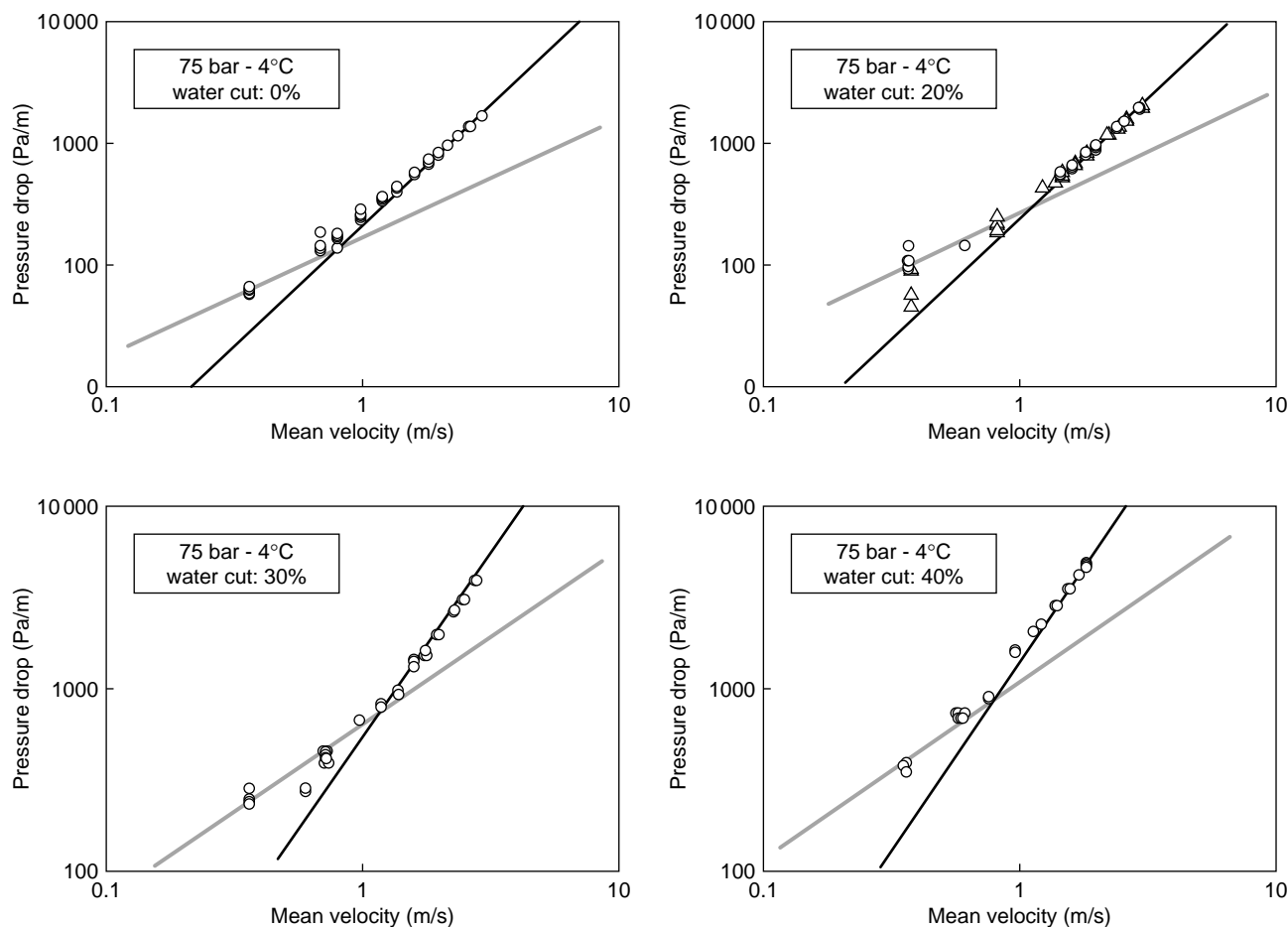


Figure 12

Pressure drop *versus* velocities in a log-log representation. Grey line is a line of slope 1 and dark line is a line of slope 2.

the agglomeration of primary droplets leading to an increase of the effective particle volume fraction. As the two systems (condensate and naphtha) are very similar, we can consider that the evolution of the effective volume fraction depending on the initial water cut is equivalent. Because of a lack of accuracy in its determination, we will present in the following results in terms of initial water cuts (defined as the volume fraction of hydrate particles) for practical reasons.

For the two systems tested, we see that a large part of the liquid flow rate imposed creates a turbulent flow. For that velocity range, roughly between 1 m/s and the maximum velocity in the loop the friction factor is constant and does not depend on velocity.

This is completely in agreement with Nikuradse work and its correlation showing that for large velocity, the friction factor is imposed by the pipe roughness:

$$\frac{1}{\sqrt{f}} = 4 \log\left(\frac{D}{2\varepsilon}\right) + 3.48 \quad (15)$$

In the two sets of experiments, the same flow loop is used with the same test tube. In this condition, the roughness of the pipe wall is the same or at least quite close and so f should be the same or very close for all the experiments done. But we observe that when more and more hydrate are formed the friction factor increases with the initial water cut.

In the Figure 13, we have plotted the value of f that has been obtained from the experiments (Figs 10 and 11) with naphtha oil and condensate for the different water cut that were investigated. For the two systems, the evolution as well as the order of magnitude of f with the initial water cut seems to be equivalent.

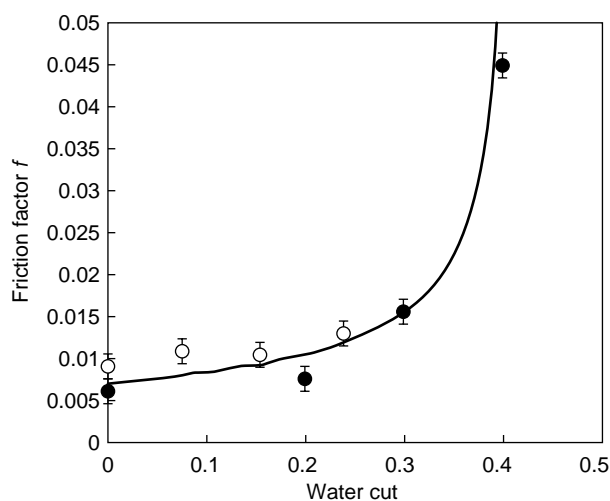


Figure 13

Variation of the friction factor f with the water cut for the two sets of experiments. White dots: naphtha oil, black dots: condensate.

Two explanations can be put forward to interpret this increase. First, we can imagine that change of the roughness at the pipe wall occurs during the hydrate formation stage as a result of a sticking process at the wall. Therefore, the pressure drop can be estimated from Nikuradse correlation if roughness is determined. But, we were not able to measure the modification of roughness at the pipe wall and we did not see, neither, any modification at the wall through the different windows of the flow loop, so this first mechanism has to be confirmed.

A second interpretation can be done related to the presence of solid particles in the fluid. These particles can contribute to the force balance and play a role in the pressure drop evaluation via friction or collisions of the particles at the wall. In that case, f should depend on the amount of particles in the system, and this is in good agreement with Figure 13.

More experimental investigations should be done to confirm the first or the second explanation. However a first conclusion is that formation of hydrate particles modify the turbulent friction factor and this modification does depend on solid amount. At high water cut the friction factor diverges.

The same variation of f with the water cut for two systems seems to indicate a close mechanism, which depend only slightly on the based fluid.

CONCLUSION

Hydrate issue becomes critical with the development of deep and ultra deep-water fields. As mentioned, conventional prevention methods reached their limits and the new options like “kinetic inhibitors” or “antiagglomerant” additives seem to be a reliable alternative in the near future. The concentration required is very low and so storage facilities and processing costs will be much lower with these techniques. But then, studies of the influence of hydrate particles on the flow properties become essential to control the flow assurance with AA additives.

The increase of pressure drop that occurs when hydrates are formed in pipelines is controlled by the friction factor under turbulent flow conditions or by apparent viscosity of the suspension in the laminar flow regime. We have tried in this article to characterize flowing properties of hydrate particles dispersed in oils in both regimes to consider the whole range of transport velocities.

In the laminar flow regime, predictions of the viscosity can be done based on hard sphere models with interactions. We showed that Newtonian behaviour is expected in most cases, and the relative viscosity of the suspension increases with the volume fraction of hydrate. In some specific cases, if interparticle forces can be high enough, shear thinning behaviour can be observed and modeled by introducing an effective volume fraction depending on aggregation rate. However, the agglomeration process which can occur during

the formation stage is complex and makes difficult the prediction of the size, shape and porosity of the hydrate particles.

In turbulent flow regime, the pressure drop is characterized by a friction factor that does not depend on velocity. For two different oils, naphtha oil and condensate, we measured experimentally the friction factor for the suspensions. We observed an increase of the friction factor with the water cut and very close values have been found for both systems. This seems to indicate that particles of hydrate play an equivalent role in both systems. This role could be an increase of the apparent roughness at the wall due to particle deposition at the formation stage or it could be an effect of the solid particles itself in modifying the force balance by hitting or moving at the wall.

We stressed also that for low viscosity oil, like condensate, settling process might occur at low velocities before we reach the laminar regime. So rheology become a non-pertinent approach to predict the flow properties. A stratified model with a bed of particles and a layer of fluid above is a better description of that situation.

REFERENCES

- Sloan, E.D. (1998) Gas Hydrates: review of physical chemical properties; *Energy and Fuels*, **12**, 191-196.
- Sloan, E.D., (1998) *Clathrate Hydrates of Natural Gases*, 2nd, Edn, Marcel Dekker, INC, New York, USA.
- Makagon, Y. (1997) *Hydrates of Hydrocarbons*, PennWell Books, Tulsa, USA.
- Englezos, P. (1993) Clathrate Hydrates, *Ind. Eng. Chem. Res.* **32**, 1251-1274.
- Makagon, Y., (1997) Recent Research on Properties of Gas Hydrates. *OTC 8299*, Houston, May 5-8, 1997.
- Lang, P.P., Rainey, R.M. and Bankston, C.H., (1998) Mensa Project: System Design and Operation. *OTC 8577*, Houston, May 1998.
- Bruinsma, D.F.M., Noltz, P.K., Desens, J.T. and Sloan, E.D., (2003) Methanol Losses to the Hydrocarbon Phases in Offshore Pipelines and its Effect on Economics. *Paper SPE 84040* presented at the *SPE Annual Technical Conference and Exhibition*, Denver, Colorado, 5-8 october 2003.
- Urdahl, O. *et al.* (1995), Inhibition of Gas Hydrate by Means of Chemical Additives. *Chem. Eng. Sci.*, **50**, 5, 863-870.
- Palermo, T. *et al.* (1997) Pilot Loop Tests of New Additives Preventing Hydrate Plugs Formation. In: *Multiphase 97, 8th International Conference on Multiphase Flow*, 133-137.
- Lederhos, J.P. *et al.* (1996) Effective kinetic inhibitors for natural gas hydrates. *Chem. Eng. Sci.*, **51**, 8, 1221-1229.
- Sinquin, A. (1999) A Global Research Program on Hydrates Control: Role of Kinetic Inhibitors. In: *3rd International Conference on Gas Hydrates*, Park City, Utah, July 18-22, 1999.
- Sugier, A., Bourgmayer, P., Behar, E. and Freund, E., (1990) Method of Transporting a hydrate Forming Fluid. *US Patent* 4, 915, 176.
- Corrigan, A., Duncum, S.N., Edwards, A.R. and Osborne, C.G. (1995) *SPE 30696* presented at the *SPE Annual Technical Conference and Exhibition*, Dallas, Oct. 22-25, 1995.
- Talley, L.D. and Mitchel, G.F. (1999) Application of Proprietary Kinetic Hydrate Inhibitors in Gas Flowlines. *OTC 11036*, Houston, May 1999.
- Palermo, T., Argo C.B, Goodwin, S.P. and Henderson, A.(1999) Flow Loop Tests on a Novel Hydrate Inhibitor to be Deployed in the North Sea ETAP Field. In: *3rd International Conference on Gas Hydrates*, Park City, Utah, July 18-22, 1999.
- Mehta, A.P., Herbert, P.B., Cadena, E.R. and Weatherman, J.P. (2002) Fulfilling the Promise of Low Dosage Hydrate Inhibitors: Journey from Academic Curiosity to Successful Field Implementation. *OTC 14057*, Houston, Texas, 6-9 May 2002.
- Frostman, L.M. and Przybylinski, J.L., (2001) Successful Applications of Anti-Agglomerant Hydrate Inhibitors. *Paper SPE 65007* presented at the *SPE International Symposium on Oilfield Chemistry*, Houston, Texas, 13-16 February 2001.
- Leporcher, E. *et al.* (1998) Multiphase Transportation: Hydrate Plugging Prevention Through Crude Oil Natural Surfactants. *Paper SPE 49172* presented at the *SPE Annual Technical Conference and Exhibition*, New Orleans, 27-30 September 1998.
- Camargo, R., Palermo, T., Sinquin, A. and Glénat, P. (1999) Rheological characterization of hydrate suspensions in oil dominated systems. *Proceedings of the 3rd International Conference on Gas Hydrates*, Salt Lake City, Utah, USA. *Annals of the New York Academy of Sciences* (2000) **912**, G.D. Holder and P.R. Bishnoi, Ed.
- Baugh, B.F. *et al.* (1997) Testing and Evaluation of Coiled Tubing Methods to Remove Blockages from Long Offset Subsea Pipelines. *OTC 8524*, Houston, May 1997.
- Minami, K. *et al.* (1999) Ensuring Flow and Production in Deepwater Environments. *OTC 11035*, Houston, May 1999.
- Gjertsen, L.H. *et al.* (1997) Removal of a Gas-hydrate Plug from a Subsea Multiphase Pipeline in the North Sea. In: *Multiphase 97, 8th International Conference on Multiphase Flow*, 515-526.
- Xiao, J.J., Hatton, G. and Kruka, V. (1997) Predicting Hydrate Plug Movement During Subsea Flowline Depressurization Operations. *OTC 8728*, Houston, May 1998.
- Camargo, R., Palermo, T., Maurel, P. and Bouchard, R. (2000) Flow properties of hydrate suspensions in asphaltenic crude oil. *Proceedings of the 2d International Conference on Petroleum Phase Behavior and Fouling*, Copenhagen, Denmark.
- Camargo, R. (2001) Propriétés rhéologiques de suspensions d'hydrate dans des bruts asphalténiques. *PhD Thesis*, University Paris VI, Paris.
- Camargo, R. and Palermo, T. (2002) Rheological Properties of Hydrate Suspensions in an Asphaltenic Crude Oil. *Proceedings of the 4th International Conference on Gas Hydrates*, May 19-23, 2002. Yokohama Symposia, Yokohama, Japan.
- Mills, P. (1985) Non-Newtonian behaviour of flocculated suspensions. *Journal de Physique – Lettres*, **46**, L301-L309.
- Jullien, R. (1990) The application of fractals to investigations of colloidal aggregation and random deposition. *New journal of chemistry*, **14**, 3.
- Potantin, A.A. (1990) On the mechanism of aggregation in the shear flow of suspensions. *Journal of Colloid and Interface Science*, **145**, 1.
- Gmachowski, L. (2000) Estimation of the dynamic size of fractal aggregates. *Colloids and Surfaces A*, **170**, 209-216.

- 31 Hoekstra, L.L., Vreeker, R. and Agterof, W.G.M. (1992) Aggregation of colloidal nickelhydroxycarbonate studied by light scattering. *Journal of Colloid and Interface Science*, **151**, 1.
- 32 Mühle, K. (1993) Floc stability in laminar and turbulent flow. In: *Coagulation and Flocculation: Theory and Applications* (B. Dobias, Ed.), Surfactant Science Series, **47**, Chap. 8.
- 33 Israelachvili, J. (1992a) Van der Waals Forces between Surfaces. In: *Intermolecular & Surface Forces*, 2nd ed., Academic Press, Chap. 11.
- 34 Herri, J.M., Gruy, F., Pic, J.S., Cournil, M., Cingotti, B. and Sinquin, A. (1999) Interest of in-situ turbidimetry for the characterization of methane hydrate crystallization: Application to the study of kinetic inhibitors. *Chemical Engineering Science*, **54**, 1849-1858.
- 35 Maurel, P., Palermo, T., Hurtevent, C., Peytavy, J.L. (2002) Shut-down/restart tests with an acidic crude under hydrate formation conditions for a deepwater development. In: *Proceedings of the 13th International Oil Field Chemistry Symposium*, 17-20 March, Geilo, Norway.
- 36 Austvik, T., Xiaoyun, L., and Gjertsen, L.H. (1999) Hydrate plug properties: Formation and removal of plugs. *Proceedings of the 3rd International Conference on Gas Hydrates*. Salt Lake City, Utah, USA. *Annals of the New York Academy of Sciences* (2000), **912** (G.D. Holder & P.R. Bishnoi, Ed.).
- 37 Peysson, Y., Nuland, S., Maurel, Ph. and Vilagines, R. (2003) Flow of hydrates dispersed in production lines. *Paper SPE 84044* presented at the 2003 *SPE Annual Technical Conference*, Denver OK.
- 38 Govier, G.W. and Aziz, K. (1972) *The flow of complex mixture in pipes*. Von Nostrand Reinhold Company.
- 39 Peysson, Y., Maurel, Ph. and Vilagines, R. (2003) Hydrate transportability in multiphase flow. Presented at the *BHRG Multiphase International Conference*, San Remo, Italy, June 2003.

Final manuscript received in December 2003

Copyright © 2004, Institut français du pétrole

Permission to make digital or hard copies of part or all of this work for personal or classroom use is granted without fee provided that copies are not made or distributed for profit or commercial advantage and that copies bear this notice and the full citation on the first page. Copyrights for components of this work owned by others than IFP must be honored. Abstracting with credit is permitted. To copy otherwise, to republish, to post on servers, or to redistribute to lists, requires prior specific permission and/or a fee. Request permission from Documentation, Institut français du pétrole, fax. +33 1 47 52 70 78, or revueogst@ifp.fr.